Auton Robot (2008) 25: 317–330
DOI 10.1007/s10514-008-9096-5

Design and control of a planar bipedal robot ERNIE with parallel knee compliance

T. Yang · E.R. Westervelt · J.P. Schmiedeler · R.A. Bockbrader

Received: 8 October 2007 / Accepted: 12 June 2008 / Published online: 9 July 2008

Abstract This paper presents the development of the planar bipedal robot ERNIE as well as numerical and experimental studies of the influence of parallel knee joint compliance on the energetic efficiency of walking in ERNIE. ERNIE has 5 links—a torso, two femurs and two tibias—and is configured to walk on a treadmill so that it can walk indefinitely in a confined space. Springs can be attached across the knee joints in parallel with the knee actuators. The hybrid zero dynamics framework serves as the basis for control of ERNIE's walking. In the investigation of the effects of compliance on the energetic efficiency of walking, four cases were studied: one without springs and three with springs of different stiffnesses and preloads. It was found that for low-speed walking, the addition of soft springs may be used to increase energetic efficiency, while stiffer springs decrease the energetic efficiency. For high-speed walking, the addition of either soft or stiff springs increases the energetic efficiency of walking, while stiffer springs improve the energetic efficiency more than do softer springs.

Keywords Bipedal robot · ERNIE · Design · Control · Walking · Parallel knee compliance · Energetic efficiency of walking

Electronic supplementary material The online version of this article (http://dx.doi.org/10.1007/s10514-008-9096-5) contains supplementary material, which is available to authorized users.

T. Yang
Digital Technology Laboratory Corporation, 950 Riverside Parkway, Suite 90, West Sacramento, CA 95605, USA
e-mail: tyang.1039@gmail.com

E.R. Westervelt (✉)
General Electric Global Research Center, One Research Circle, Niskayuna, NY 12309, USA
e-mail: Westervelt@ge.com

J.P. Schmiedeler
Department of Mechanical Engineering, The Ohio State University, Columbus, OH 43210, USA
e-mail: schmiedeler.2@osu.edu

R.A. Bockbrader
Palmer Associates, Machine Engineering & Systems Design, 4401 Jackman Rd, Toledo, OH 43612, USA
e-mail: RBockbrader@palmerassoc.com

1 Introduction

For more than three decades, the field of bipedal locomotion has been receiving increasing research interest with many bipedal robots having been built at labs around the world. In Japan, WABOT-1 (Kato and Tsuiki 1972) was constructed in the 1970s, and the recent success of ASIMO (Sakagami et al. 2002) indicates that research in bipedal locomotion remains active and strong. In Europe, several projects are active. At the Technical University Munich, Germany, JOHNNIE (Loffler et al. 2004) was designed and built. At the Delft Biorobotics Laboratory (Wisse et al. 2005, 2001; Collins et al. 2005) in the Netherlands, a series of bipeds were built based on passive walking principles (McGeer 1990). At the Laboratoire d'Automatique de Grenoble, France, a robot named RABBIT (Chevallereau et al. 2003) was constructed and served as the testbed on which the hybrid zero dynamics (HZD) approach to control biped walking (Westervelt et al. 2004) was first experimentally validated. In the United States, there have been comparatively fewer projects. At Cornell there have been several passive biped projects (Coleman and Ruina 1998; Collins et al. 2001, 2005). At MIT, the strong tradition of the MIT Leg Lab, including the notable Spring Flamingo (Pratt and Pratt 1998), has been

continued by the Robot Locomotion Group (Collins et al. 2005).

One of the most promising uses of bipedal robots is as service machines that assist humans in obstacle-ridden environments, such as the home. In such applications, where a tether is impractical, a bipedal robot will most likely rely on its on-board power supply, such as batteries. Therefore, energy efficiency is of crucial importance for bipedal robots. Various approaches have been taken to create an energetically-efficient bipedal robot.

One design-oriented approach is passive-dynamic walking wherein the robot's dynamics are designed such that the robot is able to walk stably down shallow slopes without the need for control or energy input aside from that coming from gravity (McGeer 1990; Garcia et al. 2000). This approach has been used at both Delft and Cornell, as mentioned above. There are three primary drawbacks of passive-dynamic walkers (Kuo 2007): they are only able to walk down slopes, their gaits are restricted to the few admitted by their dynamics, and they are sensitive to perturbations. Realizing these limitations, researchers have sought to improve passive-dynamic walkers by adding actuation (Collins et al. 2005).

The second approach to obtaining energetically-efficient bipedal walking is the use of mechanical compliance. In Farrell et al. (2007), Collins and Ruina (2005), Anderson et al. (2005), springs were added at the passive ankles to improve the energetic efficiency of walking. In Iida et al. (2005), springs were added across the hip and shank, and thigh and heel simultaneously. Series-elastic actuation was implemented on Spring Flamingo to enable control of the ground reaction forces in walking, thus providing an active suspension (Pratt et al. 2001). Vanderborght et al. (2006) used McKibben's muscles as a means to add controllable joint compliance. Compliant elements have also been used in the design of hopping and running bipeds, such as the pioneering work of Raibert (1986), and more recently by Ahmadi et al. (1999) and Hurst et al. (2007).

The third approach to obtaining energetically-efficient bipedal walking is the design of gaits that minimize the energetic cost of walking. The most common means of design is to use parametric optimization to choose the parameters that specify the gait of the robot. For example, Chevallereau et al. (2001) used parametric optimization to design fourth-degree polynomial functions that give the joint motions over a step as functions of time. In another example, Channon et al. (1992) used parametric optimization to design third-degree polynomial functions that give the motions of the hip and swing foot of the robot as a function of time, and the corresponding joint trajectories were determined by an inverse kinematic model of the robot. Unlike the previous two examples in which each reference trajectory was described by a single polynomial function of time, in Saidouni and Bessonnett (2003) cubic splines connected at points uniformly distributed along the "motion time" are used to generate complete optimal steps, including a double-support phase. Another means of designing gaits that minimize the energetic cost of walking is by application of Pontryagin's Maximum Principle (PMP). The first application of PMP to gait generation can be found in Chow and Jacobson (1971). More recently, Rosatami et al. (1998, 2001) used PMP to design impact-less gaits by casting the constrained gait optimization problem as a two-point boundary value problem. Different from these methods based on off-line model-based optimization, gait generation based on learning is also a common approach. Capi et al. (2003) enabled real-time gait generation with a neural network designed using learning. Tedrake (2005, 2004) used online learning to continuously adapt the gait.

This paper contributes to the literature on energetically-efficient bipedal robots by presenting the design and control of the planar bipedal robot ERNIE, which was designed and constructed at The Ohio State University. ERNIE was constructed to serve as a testbed for the study of the influence of design and control on the performance of bipedal walking. Its purposefully simple morphology—two legs with knees, no feet, and a torso—was inspired by that of RABBIT. Unlike RABBIT, ERNIE has two design features that enable a range of experiments: compliance may be added at the knees in parallel with the actuators, and its legs are modular. ERNIE's control system is based on the HZD framework (Westervelt et al. 2007) wherein gaits are designed using parametric optimization. The paper also presents numerical and experimental studies of the effects of adding parallel knee joint compliance on the energetic efficiency of walking.

The remainder of the paper is organized as follows: Sect. 2 presents ERNIE's system specifications and mechanical design. Section 3 describes issues related to system integration. Section 4 summarizes the control approach. Section 5 presents a numerical study of the influence of knee compliance on the energetic efficiency of walking, and Sect. 6 presents the corresponding experiment results. Conclusions are drawn in Sect. 7.

2 Mechanical design

ERNIE is a planar biped composed of 5 links: a torso, two femurs and two tibias. The two hip and two knee joints are all actuated revolutes. To restrict ERNIE's walking motion to its sagittal plane, a boom is attached to the torso via an unactuated revolute joint coaxial with the hips. The revolute connection allows for the body to pitch relative to the boom. Figure 1 is a photograph of ERNIE's experimental setup when ERNIE is on a treadmill. Table 1 gives ERNIE's geometric and inertial parameters as determined

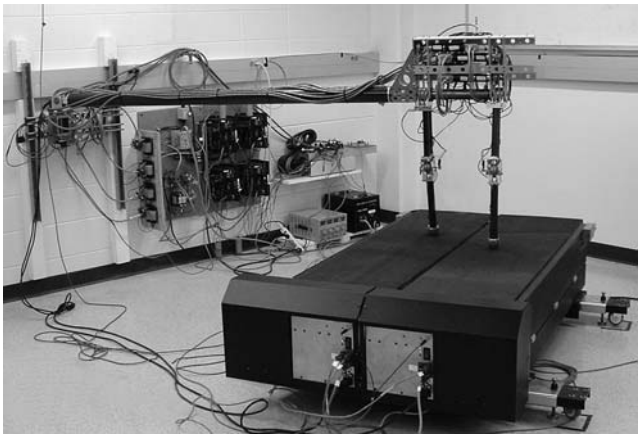

Fig. 1 The biped prototype ERNIE's experimental setup

Table 1 Link parameters for ERNIE

Model parameter	Units	Link	Value
Mass	kg	torso	13.6
		femur	1.5
		tibia	1.0
Length	m	torso	0.28
		femur	0.36
		tibia	0.36
Mass center[a]	m	torso	0.14
		femur	0.13
		tibia	0.12
Inertia[b]	kg·m^2	torso	0.09
		femur	0.02
		tibia	0.02
Motor rotor inertia	kg·m^2	–	2.09×10^{-5}
Gearhead ratio	–	–	91
Gearhead inertia	kg·m^2	–	1.5×10^{-6}

[a]The mass center of each link is measured along the link axis from the nearest joint

[b]The link inertia is measured with respect to its mass center

from a solid model assembly composed of the individual parts from which all of the specialized components were manufactured.

2.1 Features of the mechanical design

The following are the key features of ERNIE's mechanical design.

Parallel compliance at the knees With a simple cable-mounting assembly at the knee joints, extension springs can be easily added across the knee joints in parallel with the actuators. The addition of compliance has the potential to improve the energetic efficiency of walking. This design feature was inspired by Alexander's (1999) idea that it is possible to reduce the work done by the actuators by using return springs to decelerate the leg at the end of each forward or backward swing, and accelerate the leg in the other direction.

Modular legs The mechanical couplings at the knee joints and hip joints are designed to make the femurs and tibias independent modules. With this modular design, the leg lengths and leg ends may be changed with minimal redesign. In this way, modularity facilitates future studies involving mechanical changes such as walking with feet.

Low-mass links ERNIE's boom and legs are made primarily of carbon fiber to reduce the total mass without compromising structural rigidity.

Actuators in the torso Locating all of the actuators in the torso reduces the mass that is distal to the robot's mass center. The result is lighter legs, thus reducing the power requirements and allowing for smaller motors to be used.

2.2 Limb and torso design

Femur and tibia design To minimize high-order modes of the robot's mechanics, the robot's legs were designed to be stiff. Carbon fiber tubing was used for the tibias and femurs because of its high rigidity and strength-to-weight ratio. Each limb segment is composed of two tubes. The tube ends are bonded to aluminum plugs that fit inside the tubes. The two carbon fiber tubes of each femur (28.7 mm OD and 1.6 mm wall thickness) are spread apart from the neutral bending axis, while the two carbon fiber tubes of each tibia (28.7 mm and 32.1 mm ODs and 1.6 mm wall thickness) are aligned concentrically. The bending moment on the femur is larger than that on the tibia during stance, so greater strength is needed in the femur. The concentric arrangement of the tubes in the tibia modestly increases its bending resistance without increasing its width in the sagittal plane. A wide tibia would create ground interference problems because the foot, described below, is directly attached to the end of the tibia. The femurs and tibias have the same length of 0.36 meters, and their length ratio approximately equals the length ratio of a human's femur and tibia (Gunther and Ruder 2003). This design enables ERNIE to walk like a human. Human-like walking in bipedal robots is of particular interest for their adoption in human-oriented environments.

Torso design The torso was designed to house the motors, connect to the boom, and generally provide structure for the robot as a whole. The torso is made of 6.35 mm (0.25 inch) aluminum plate because of its combination of machinability, structural stiffness, and light weight.

Foot design ERNIE's feet are hemispherical and designed to provide an unactuated degree of freedom in the sagittal plane between the tibia and the ground. Each aluminum hemisphere is covered with half of a racquet ball to provide cushioning at ground impact as well as to increase the coefficient of friction between the foot and the walking surface. With this covering, the foot radius is about 30 mm. A force sensitive resistor is placed between the foot and tibia and is used to detect foot-ground contact. ERNIE's feet are attached to the ends of the tibias via simply assemblies. This modular design minimizes the mechanical coupling between the feet and the tibias, and the hemispherical feet can be replaced easily for other studies, such as walking with curved feet.

2.3 Actuation and transmission

Actuation Since the weight of the actuators accounts for a significant portion of the total weight of the biped, it is important to choose actuators with a high power-to-weight ratio. As a result, brushless DC motors were chosen for ERNIE with the size determined from simulations of a detailed model of the robot walking under closed-loop feedback control. Using these simulations, the design of ERNIE was iterated until the needed components' specifications matched those that were available off the shelf. The following motors from Maxon Precision Motors Inc. were chosen: brushless DC motor EC45-136212 combined with motor gearhead GP42C-203125 (91:1 ratio) and the incremental encoder HEDL 9140 (500 lines per revolution). The motors are powered by brushless servo amplifier B60A40AC from Advanced Motion Controls.

Transmission Since all of the motors are located in the torso, transmissions are needed to transmit power from the motors to the joints. Wire rope cabling (7X19 with uncoated OD of 3.2 mm and vinyl coated for a total OD of 4.8 mm) is combined with pulleys (63.5 mm diameter) to give a simple, compact, and light transmission. For the knee joint transmissions, additional idler pulleys are used at the hips. The pulleys feature slip rings that have a running fit about the pulley body packed with grease. This design allows both halves of the cables to have relative motion during cable tensioning.

Parallel energy storage Extension springs can be mounted across the knee joints in parallel with the actuators as shown in Fig. 2. The design allows for two extension springs to be attached in parallel across each knee joint to achieve a relatively high effective stiffness without employing an unduly large spring. One end of each extension spring is attached at the top of the femur assembly, and the other end is attached to a wire rope using a wire rope thimble. The wire rope wraps around a circular cam of radius r that is rigidly

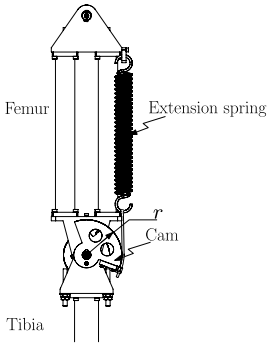

(a) Schematic of springs in parallel with knee joint actuators

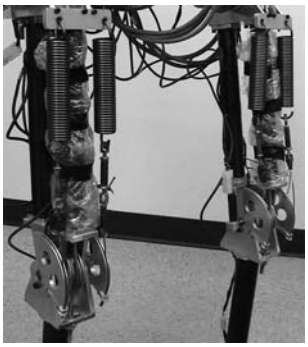

(b) Actual assembly of springs in parallel with knee joint

Fig. 2 Springs in parallel with knee joint

fixed to the tibia. Since the cam is circular, the torque applied to the knee joint is linearly related to the knee's angular displacement. With this design, the knee springs engage only when the knee joints flex to a certain angle, which is termed the knee spring offset. The overall wire rope length can be adjusted with an in-line turnbuckle or a cable stop as shown in Fig. 2(b). Hence, the knee spring offset can be adjusted by changing the wire rope length.

When the selected extension springs have a nonzero preload $F^{0,l}$ and constant spring stiffness K^l_{sp}, the equivalent torsional spring stiffness K_{sp} and the equivalent torsional spring preload τ^0 are

$$K_{sp} := 2K^l_{sp} r^2, \tag{1a}$$

$$\tau^0 := 2F^{0,l} r. \tag{1b}$$

The use of parallel compliance does not increase the control design complexity, as would the addition of series compliance.

2.4 ERNIE's experimental setup

To provide frontal plane stabilization, a boom is attached to ERNIE with a revolute joint and to the wall with a pair of intersecting revolute joints. The three revolute joints of the boom system intersect at a single point.

Due to limited lab space, ERNIE is configured to walk on a treadmill. The treadmill has a split track. ERNIE is located such that only one leg falls on each track. With this configuration, the potential for coupling in the legs' motions due to lateral compliance in the track is minimized.

3 System integration

3.1 Sensors and computation

As an experimental biped, ERNIE has a large sensor set installed. Each actuated joint is equipped with a 5 kΩ poten-

tiometer (Clarostat Sensors and Controls model 308 NPC) that is attached to the shaft of the joint to measure the joint's angular displacement. A potentiometer of the same type is used to measure the torso angle with respect to the boom. Encoders are attached directly to the shafts of each motor to measure the motor shaft's angular displacement. Two additional encoders (CUI Inc. model NSO-S10000-2MD-10-050) are used to measure the boom angular positions in the vertical and horizontal planes. For each track of the treadmill, an encoder signal is provided from the treadmill to measure the distance traveled. This signal is used to compute ERNIE's relative position with respect to the treadmill.

To detect ground contact, a force sensitive resistor (FSR) is inserted between the foot and tibia of each leg in such a way that the pressure on the FSR increases when the foot is on the ground. A voltage divider is used to measure the change in pressure. Since the pressure measurement suffers from significant drift, the signal is numerically differentiated, and detection of foot touchdown is based on a threshold of the differentiated signal.

ERNIE's real-time control platform is a dSPACE DS1103 system. This system features a PowerPC 604e processor running at 400 MHz, 2 MB SRAM local memory, and 128 MB SDRAM global memory. Other features include 20 ADC channels, 8 DAC channels, 6 digital incremental encoder channels, and 32 bits of digital I/O.

3.2 Robot–treadmill interaction

Lateral compliance of the treadmill belts provides a restorative torque that helps to stabilize the average position of ERNIE on the treadmill when walking. Figure 3 depicts a top view of ERNIE walking on its treadmill with the inner leg as the stance leg. Over a step, the desired average value of ϕ_h, the angle between the boom axis and the normal to the treadmill tracks, is zero. That is, the desired average orientation of the robot's sagittal plane over a step is parallel to the treadmill's direction of progression. Since the leg ends

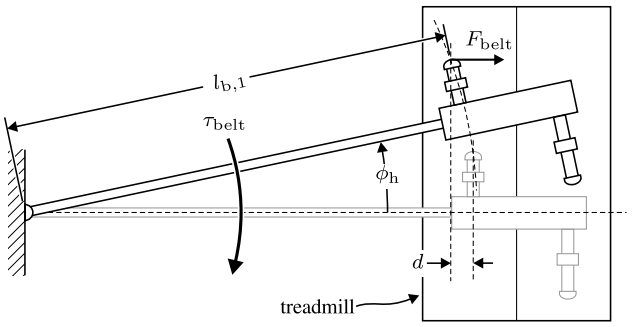

Fig. 3 Top view of ERNIE's experimental setup. Lateral compliance in the treadmill belts provides a restorative torque that tends to keep the robot's sagittal plane aligned with the treadmill. The position of ERNIE when $\phi_h = 0$ is depicted in *gray*

do not readily slip on the treadmill surface because of the foot covering, when $\phi_h \neq 0$ the lateral compliance of the treadmill belts provides a restorative torque that may be approximated as follows.

Assume that the treadmill belts have a lateral stiffness of k_{belt}. The force experienced at the stance leg end in the lateral direction of the treadmill may be approximated as

$$F_{\text{belt}} \approx k_{\text{belt}} d = k_{\text{belt}} l_{b,1}(1 - \cos(\phi_h)). \tag{2}$$

Thus, the restorative torque may be approximated as

$$\tau_{\text{belt}} \approx F_{\text{belt}} l_{b,1} \sin(\phi_h) = k_{\text{belt}} l_{b,1}^2 \sin(\phi_h)(1 - \cos(\phi_h)). \tag{3}$$

This torque acts to stabilize the average position of the robot when walking on the treadmill.

4 Control overview

ERNIE's control system is based on the HZD framework (Westervelt et al. 2007). To maximize the benefits of adding parallel knee joint compliance, the gaits and the spring parameters must be chosen appropriately. This selection may be done via simultaneous optimization of the gait and the spring parameters.

4.1 ERNIE's dynamic model

It is assumed that a normal step consists of an instantaneous double support phase, when both legs are in contact with the ground, and a single support phase, when only one leg end is in stationary contact with the ground. The alternation of these two phases results in a hybrid model of walking.

During the single support phase, the robot is modeled as a 5-link rigid-body mechanical system. The equations of motion are

$$D(q)\ddot{q} + C(q, \dot{q})\dot{q} + G(q) + E(q) = Bu, \tag{4}$$

where $q := (q_1; \ldots; q_5) \in \mathcal{Q}$ are the joint angles (see Fig. 4), $\mathcal{Q}$ is a simply-connected, open subset of $[0, 2\pi)^5$, $\dot{q} \in \mathbb{R}^5$, and $u \in \mathbb{R}^4$. Since the dimension of u is smaller than the dimension of q, the robot is underactuated. The matrix $D(q)$ is the mass-inertia matrix, $C(q, \dot{q})$ is the matrix of centripetal and Coriolis terms, $G(q)$ is the gravity vector, and B is the input matrix. The vector function $E(q)$ describes the torques supplied by the springs at the knee joints. In the case that no springs are attached, $E(q)$ is a 5×1 zero vector. When compliance is present at the knees, $E(q)$ is given by

$$E(q) := (0;\ 0;\ E_3(q_3);\ E_4(q_4);\ 0). \tag{5}$$

Since the springs at the knee joints are pre-loaded extension springs, they can only apply torques when they are stretched.

As a result, the torques can be described by nonlinear functions,

$$E_i(q_i) := \begin{cases} K_{sp}(q_i - q^0) + \tau^0, & q_i \le q^0 \\ 0, & q_i > q^0, \end{cases} \tag{6}$$

where $i = 3, 4$, K_{sp} is the equivalent spring stiffness constant given by (1a), τ^0 is the equivalent spring preload given by (1b), and q^0 is the spring offset. As the knee joint rotates from zero offset in the negative sense, the springs will engage at a chosen offset angle q^0. Once the springs engage, the torque supplied by the springs changes linearly with respect to the change in knee joint angle.

Defining $x := (q; \dot{q})$, the model written in state-space form is

$$\dot{x} = \begin{bmatrix} \dot{q} \\ D^{-1}(-C\dot{q} - G - E) \end{bmatrix} + \begin{bmatrix} 0 \\ D^{-1}B \end{bmatrix} u, \tag{7a}$$

$$=: f(x) + g(x)u, \tag{7b}$$

with state space $T\mathcal{Q} := \{(q; \dot{q}) \mid q \in \mathcal{Q}, \dot{q} \in \mathbb{R}^5\}$.

The double support phase is assumed to be instantaneous and modeled by a rigid impact (see Westervelt et al. 2003 for a complete list of hypotheses concerning the impact and model derivation). The state variables just after and just before impact are related by an algebraic map $x^+ = \Delta(x^-)$, where x^+ is the state just after the impact, and x^- is the state just before impact. The impact map is applied whenever the state enters the switching set $\mathcal{S}$ (at double support), where

$$\mathcal{S} := \left\{ (q, \dot{q}) \in T\mathcal{Q} \;\middle|\; p_2^v(q) = 0,\ p_2^h(q) > 0 \right\}, \tag{8}$$

where p_2^v and p_2^h are the position of the swing leg end with respect to the stance leg end; see Fig. 4.

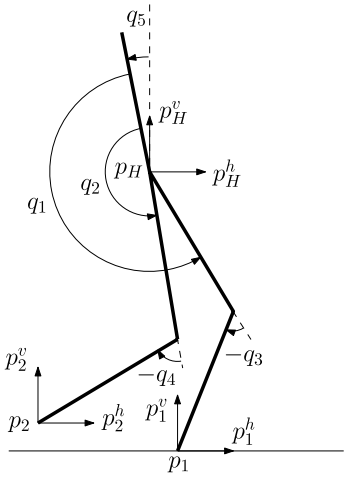

Fig. 4 ERNIE's measurement conventions as depicted from the boom-side of the robot

The overall hybrid model is given as

$$\Sigma : \begin{cases} \dot{x} = f(x) + g(x)u, & x^- \notin \mathcal{S} \\ x^+ = \Delta(x^-), & x^- \in \mathcal{S}. \end{cases} \tag{9}$$

4.2 Controlling stable dynamic walking

The control design in this paper follows the approach proposed by Westervelt et al. (2003). The approach is summarized here for completeness.

For the model (4), suppose that there exists a function $\theta : \mathcal{Q} \to \mathbb{R}$ that is monotonically increasing over the duration of a step. Define a parameterized set of holonomic constraints, $h_{d,\alpha}(\theta) : \mathbb{R} \to \mathbb{R}^4$ on the actuated coordinates, which is expressed as

$$h_{d,\alpha}(\theta) := (h_{d1,\alpha^1}; h_{d2,\alpha^2}; h_{d3,\alpha^3}; h_{d4,\alpha^4}). \tag{10}$$

The 4 constraint functions h_{di,α^i} where $i = 1, \ldots, 4$ are chosen to be Bézier polynomials,

$$h_{di,\alpha^i} := \sum_{k=0}^{M} \alpha_k^i \frac{M!}{k!(M-k)!} s^k (1-s)^{M-k}, \tag{11}$$

where $s := (\theta - \theta^+)/(\theta^- - \theta^+)$, which monotonically increases from 0 to 1 over a step, $\alpha^i := (\alpha_0^i; \ldots; \alpha_M^i) \in \mathbb{R}^{M+1}$, and θ^+ and θ^- are the values of θ at the beginning and end of the swing phase.

Let $\alpha := [\alpha^1, \ldots, \alpha^4] \in \mathbb{R}^{(M+1)\times(4)}$ and define the output

$$y = h(q) := h_0(q) - h_{d,\alpha}(q), \tag{12}$$

where $h_0(q) := (q_1; \ldots; q_4)$. The set of parameters α is said to be *regular* if it satisfies output Hypothesis HH1–HH5 given in Westervelt et al. (2003). The parameters being regular implies that the associated decoupling matrix is invertible, and there exists a two-dimensional zero dynamics during the swing phase. The associated zero dynamics manifold $\mathcal{Z}_\alpha := \{x \in T\mathcal{Q} \mid h(x) = 0, L_f h(x) = 0\}$ is rendered invariant by the feedback control $u^*(x) := -(L_g L_f h(x))^{-1} L_f^2 h(x)$. Let the feedback control Γ_α be any feedback control satisfying Hypothesis CH2–CH5 given in Westervelt et al. (2003). Then, $\mathcal{Z}_\alpha$ is invariant under Γ_α and is locally finite-time attractive. Furthermore, the HZD exists if $\Delta(S \cap \mathcal{Z}_\alpha) \subset \mathcal{Z}_\alpha$.

Let (ξ_1, ξ_2) be coordinates for $\mathcal{Z}_\alpha$ where $\xi_1 := \theta$, $\xi_2 := \partial K/\partial \dot{q}_5|_{\mathcal{Z}_\alpha} = d_5(q)\dot{q}$ and where $K(q, \dot{q}) = \frac{1}{2}\dot{q}' D \dot{q}$ is the kinetic energy of the robot and d_5 is the row of D corresponding to the absolute coordinate. In these coordinates, the HZD takes the form

$$\begin{cases} \begin{bmatrix} \dot{\xi}_1 \\ \dot{\xi}_2 \end{bmatrix} = \begin{bmatrix} \kappa_1(\xi_1)\xi_2 \\ \kappa_2(\xi_1) \end{bmatrix}, & (\xi_1, \xi_2) \notin (S \cap \mathcal{Z}_\alpha) \\ \begin{bmatrix} \xi_1^+ \\ \xi_2^+ \end{bmatrix} = \begin{bmatrix} \theta^+ \\ \delta^2_{\text{zero}} \xi_2^- \end{bmatrix}, & (\xi_1, \xi_2) \in (S \cap \mathcal{Z}_\alpha), \end{cases} \tag{13}$$

where δ^2_{zero} is a constant that can be readily computed, and κ_1 and κ_2 are given by

$$\kappa_1(\xi_1) = \frac{\partial \theta}{\partial q} \begin{bmatrix} \frac{\partial h}{\partial q} \\ d_n(q) \end{bmatrix}^{-1} \begin{bmatrix} 0 \\ 1 \end{bmatrix} \Bigg|_{\mathcal{Z}_\alpha} \tag{14}$$

and

$$\kappa_2(\xi_1) = -\frac{\partial V}{\partial q_n}\Bigg|_{\mathcal{Z}_alpha}, \tag{15}$$

where $V(q)$ is the potential energy of the robot.

For the hybrid system, let $\zeta_2 := \frac{1}{2}(\xi_2)^2$ and $V_{\text{zero}}(\theta) := -\int_{\theta^+}^{\theta} \kappa_2(\xi)/\kappa_1(\xi) d\xi$. Then the restricted Poincaré map $\rho : S \cap \mathcal{Z}_\alpha \to S \cap \mathcal{Z}_\alpha$ has the form

$$\rho(\zeta_2^-) = \delta^2_{\text{zero}} \zeta_2^- - V_{\text{zero}}(\theta^-), \tag{16}$$

and its domain of definition is given by

$$\left\{ \zeta_2^- > 0 \mid \delta^2_{\text{zero}} \zeta_2^- > V^{\max}_{\text{zero}} \right\}, \tag{17}$$

where $V^{\max}_{\text{zero}} := \max_{\theta^+ \le \theta \le \theta^-} V_{\text{zero}}(\theta)$.

There exists an exponentially stable periodic orbit of the HZD if, and only if,

$$\delta^2_{\text{zero}} < 1 \quad \text{and} \quad \frac{\delta^2_{\text{zero}}}{1 - \delta^2_{\text{zero}}} V_{\text{zero}}(\theta^-) + V^{\max}_{\text{zero}} < 0, \tag{18}$$

with the corresponding fixed point $\zeta_2^{*-} := -\frac{V_{\text{zero}}(\theta^-)}{1-\delta^2_{\text{zero}}}$.

A thorough treatment of the HZD and control design approach summarized in this section can found in Westervelt et al. (2007).

4.3 Control algorithm implementation

In the experiments presented in this paper, the output function is given by (11)–(12) with $\theta = [-1,\ 0,\ -1/2,\ 0,\ -1,\ ]q$. The Bézier polynomial order M was chosen to be 6. The polynomial parameters were found via constrained numerical optimization to approximately minimize the average mechanical absolute power over one step,

$$J = \frac{1}{T_I(\zeta_2^-)} \sum_{i=1}^{4} \int_0^{T_I(\zeta_2^-)} |u_i \dot{q}_i| dt, \tag{19}$$

where $T_I(\zeta_2^-)$ corresponds to the step duration.

To achieve human-like walking, the following optimization constraints were used:

Average walking rate constraint The average walking rate was constrained to be a specified value.

Ground contact constraints The normal component of the ground reaction force was constrained to point upwards, and the ratio of the tangential to normal ground reaction forces was constrained to be less than the foot-ground static friction constant to ensure that the stance foot remains on the ground and does not slip. The coefficient of maximum foot-ground static friction is 0.37 in the gait design.

Joint motion ranges, swing foot ground clearance, and step length Constraints were imposed so that the resulting walking pattern is human-like.

Required actuator power and torque Constraints were imposed to ensure that the required power and torque were within the actuators' limits.

In the HZD framework applied to ERNIE, the hip and knee joints are controlled to follow reference motions, which results in a one-dimensional HZD. The reference motions are designed via optimization so that the resulting gaits are stable and efficient. High-gain joint feedback control is used to drive y defined in (12) to zero, thus ensuring that the gaits induced match their design. Although one might expect superior performance if output feedback linearization were used, it is the experience of the authors that the performance is comparatively worse due to unmodelled system dynamics and parameter uncertainty.

During the gait design, when ERNIE's model including knee springs is used, the benefits of these springs are utilized naturally, such that when the knee joints follow the reference trajectories, these springs help to reduce the desired cost, (19).

5 Numerical study of the influence of knee springs on the energetic efficiency of walking

In this section, the influence of the knee springs on the energetic efficiency of walking is analyzed via numerical simulation. This study is inspired by the idea that the compliant elements at the knee joints may increase the energetic efficiency of walking by the cyclic storage and release of energy (Alexander 1999).

The four cases studied are given in Table 2. In Case 1, gaits were designed based on ERNIE's model without

Table 2 Optimization design cases

Case	K_{sp} (N m/rad)	τ^0 (N m)
1	0	0
2	6.19	1.73
3	16	2.74
4	20.13	2.95

Table 3 Optimization constraints used in gait design

Design constraint	Minimum	Maximum
Static friction constant	0	0.35
Swing foot height	$0.18(-s^2+s)$ m	–
Stance leg hip joint	2.1 rad (120°)	4.7 rad (270°)
Swing leg hip joint	2.1 rad (120°)	4.7 rad (270°)
Stance leg knee joint	−1.6 rad (−90°)	0 rad (0°)
Swing leg knee joint	−1.6 rad (−90°)	0 rad (0°)
Torso angle	−0.2 rad (−10°)	0.2 rad (10°)
Step length	0.15 m	0.25 m
Knee spring offset	−0.5 rad (−30°)	0.5 rad (30°)

springs. In Cases 2 through 4, gaits were designed based on ERNIE's model with three different sets of springs in parallel with the knee actuators. The spring stiffnesses were chosen using a two-step process. First, gaits were designed for a range of speeds and spring stiffnesses. Second, spring stiffnesses that resulted in low-cost walking for a range of speeds were selected according to commercial availability.

The optimization constraints used in the design of all gaits are given in Table 3. For each case, eight gaits were designed with different average walking rates varying from 0.3 m/s to 0.65 m/s in increments of 0.05 m/s.

5.1 Case 1: gaits designed without knee springs

The average power costs of the eight gaits designed without springs are given in Fig. 5. Although the step length is constrained between 0.15 m and 0.25 m, the resulting gaits all have a step length of 0.25 m. As can be seen from Fig. 5(a), the average power cost of walking without springs increases nearly quadratically with respect to the increase of the average walking rate. Similar results have been reported in Ralston (1958), Bastien et al. (2005), Browning and Kram (2005).

5.2 Cases 2 through 4: gaits designed with knee springs

In each of Cases 2 through 4, gaits were designed via simultaneous optimization of the gait and the knee spring offsets. Note that during the design, the knee spring offset was constrained between −0.5 rad (−30°) and 0.5 rad (30°). The knee joint angles were constrained between 0 rad (0°) and −1.6 rad (−90°) to prevent knee joint hyper-extension. In all three cases, the optimization design yields gaits in which the knee spring offset is such that the knee springs are slack during a portion of a step. This finding indicates that for the current system configuration, spring engagement for only a portion of the step results in higher efficiency.

Figure 6 gives the simulation result of the knee joint torque and the knee joint motion during one step with the gait designed for a walking rate of 0.65 m/s with the springs

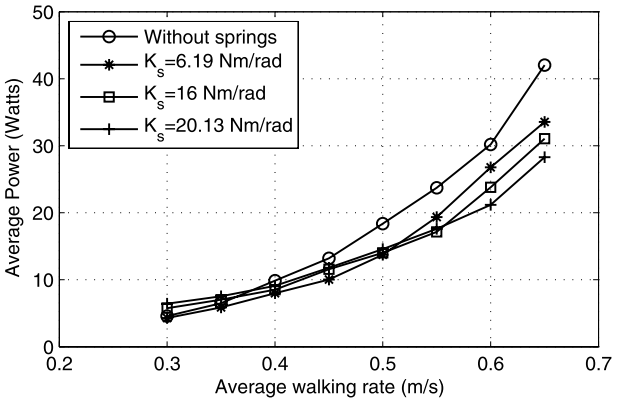

(a) Average power cost with and without springs for various speeds and spring stiffnesses

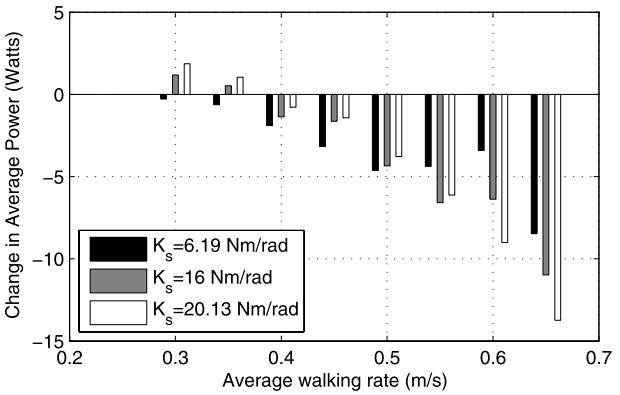

(b) Changes in average power cost with springs compared with the average power cost without springs

Fig. 5 Average power cost over one step calculated from simulation

of case 3. In Figs. 6(a) and 6(b), the lines represent the required stance knee joint torque and swing knee joint torque, respectively, with and without the springs. For this gait, the designed knee joint spring offset is −0.34 rad. When springs are added with the designed spring offset, the springs on the stance leg knee joint are slack over the entire step since the stance leg knee joint angle is always greater than −0.34 rad.

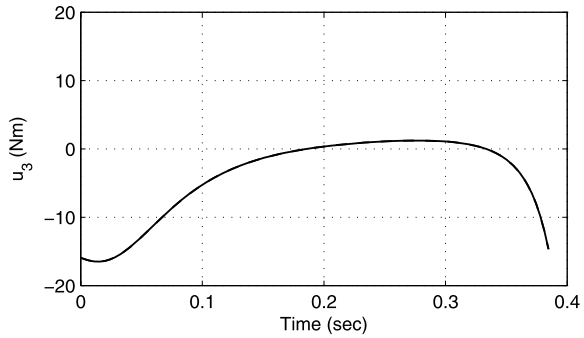

(a) Stance leg knee joint torque profiles with (solid) and without (dashed) springs. Note that the curves are coincident

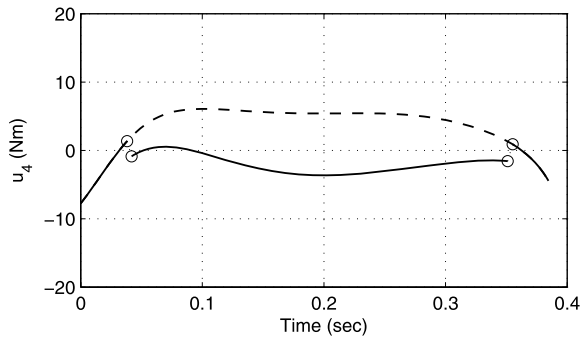

(b) Swing leg knee joint torque profiles with (solid) and without (dashed) springs. The discontinuity in the torque profile of the case with springs is due to the springs' nonzero preload

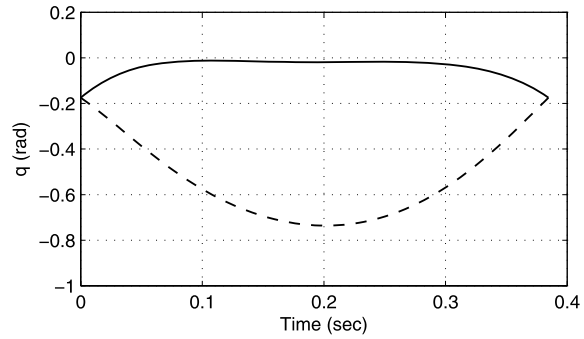

(c) Stance (solid) and swing (dashed) knee joint trajectories

Fig. 6 Knee joint torque profiles for the 0.65 m/s gait. The equivalent spring stiffness used is 16 N m/rad

The torque profiles with and without springs are therefore the same. The springs on the swing leg knee joint, on the other hand, are engaged between approximately 0.04 seconds and 0.35 seconds, when the swing leg knee joint angle is less than −0.34 rad. Consequently, the resulting torque profiles with and without springs are different during this period. As a result, the average power cost with springs is less than the average power cost without springs. The power savings is due to the reduction in the power supplied by the actuators to decelerate the swing knee.

The average power costs of the three sets of gaits designed with springs are given in Fig. 5(a). As in the case without springs, the average power cost of walking with springs increases approximately quadratically with the increase in average walking rate. At low walking rates, gaits designed for the softest spring are more efficient than walking without springs, and gaits designed for the stiffer springs are progressively less efficient with increasing spring stiffness. Conversely, at high average walking rates, gaits without springs are less efficient than gaits with springs, regardless of stiffness, and gaits designed for stiffer springs are progressively more efficient with increasing spring stiffness. This correlation is due to matching the spring deflections and knee joint torques required by the gaits; in general, faster gaits have larger joint displacements and higher torque requirements than slower gaits.

5.3 Effect of spring parameter variation on average power cost

To investigate how spring stiffness and spring preload affect walking efficiency for the given gaits using simulation, four gaits with average rates of 0.35 m/s, 0.45 m/s, 0.55 m/s, and 0.65 m/s were designed with the springs of case 3. Figure 7 plots the power cost (19) computed when the spring stiffness is varied from 0 N m/rad to 40 N m/rad and the preload from 0 N m to 5 N m.

For each of the four contour plots, a valley exists such that the average power cost is minimal at the nadir of the valley. With the average walking rate increasing from 0.35 m/s to 0.65 m/s, the valley and its nadir shift from the left bottom corner of the plots to the right and upward as shown by Figs. 7(a)–7(d). This indicates that in general, to increase the energetic efficiency of walking, the spring stiffness and preload need to be increased when the average walking rate increases, but improperly over-increasing or under-increasing these two values will diminish the benefit of energy saving provided by the parallel compliance at the knee joints. Particularly for the given four gaits with springs of case 3, the spring stiffness and preload combination is sub-optimal for all four gaits, and an optimal spring stiffness and preload combination can be estimated from Fig. 7 for the given speeds or gaits. This observation is intuitive too. In general, at a high average walking rate, the biped needs to swing its leg fast, and stiff springs can assist the motor more than soft springs. On the other hand, at a low average walking rate, the improperly stiff springs may work against the motors, increasing the average power cost of walking.

6 Experimental verification

This section describes experiments that validate the results of Sect. 5. The general experiment procedure is described first, and the results follow.

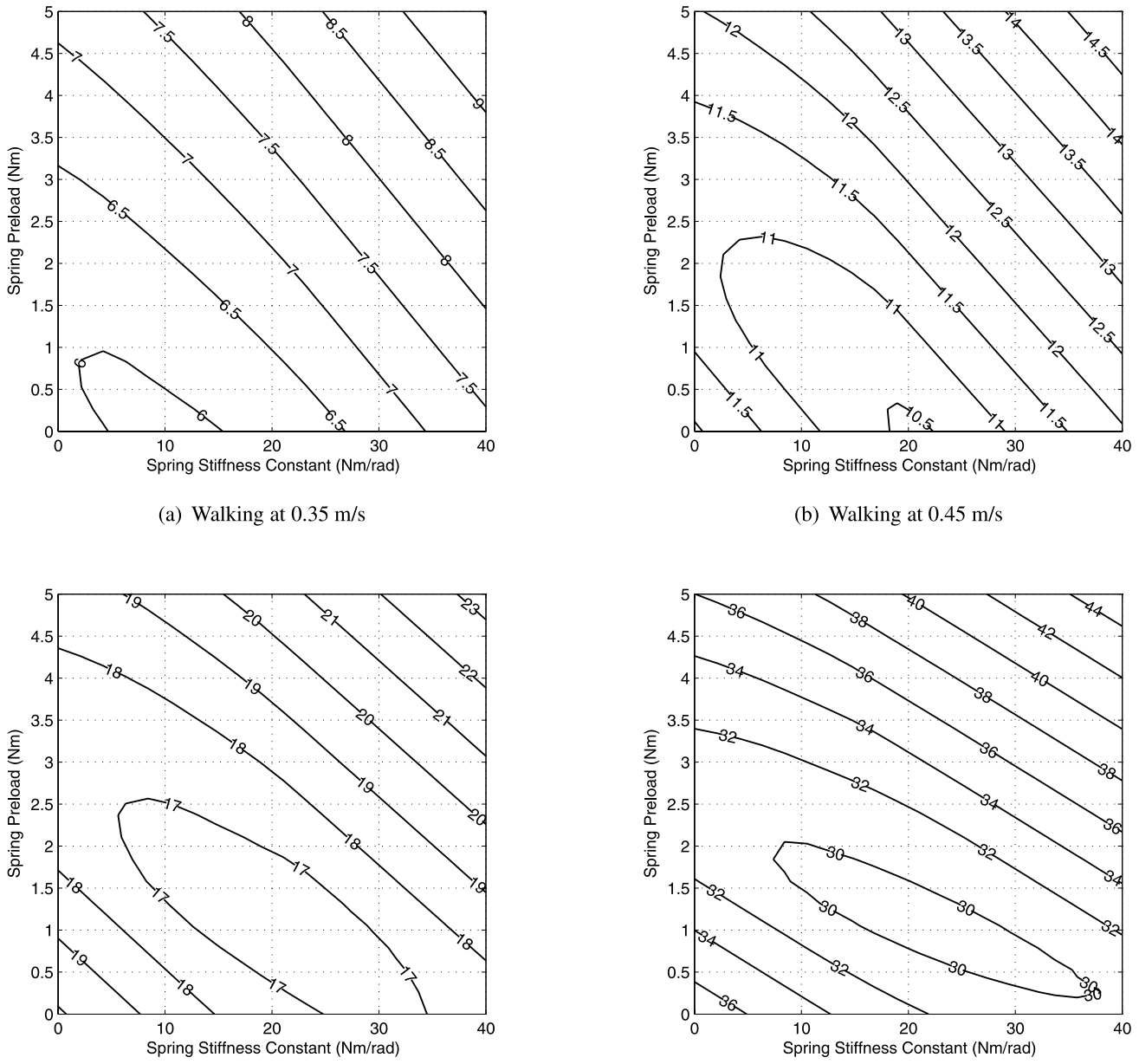

(a) Walking at 0.35 m/s

(b) Walking at 0.45 m/s

(c) Walking at 0.55 m/s

(d) Walking at 0.65 m/s

Fig. 7 Average power with respect to spring stiffness and preload for four walking rates. The gaits were designed with the spring of equivalent stiffness 16 N m/rad and preload 2.74 N m

6.1 Experiment procedure

The experiment procedures for walking without knee springs and walking with knee spring are the same aside from the need to install and adjust the springs for the latter.

The first step of the experimental procedure is to add the springs and set the spring offset as needed. The robot's potentiometers are then calibrated. Next, ERNIE is servoed to the initial configuration of the selected gait and placed on the treadmill with the treadmill at zero speed. To initiate walking, the controller is switched to the HZD-based feedback controller and an experimenter holds the robot's boom stationary while the treadmill speed is ramped up. As a consequence of the zero dynamics' parameterization by forward progression—which is relative to a frame fixed to the treadmill belt—the robot's gait naturally synchronizes with the treadmill. Once the treadmill speed matches that of the gait design, the experimenter releases the boom. To stop the robot, the experimenter grasps the boom, holding it stationary, and the treadmill speed is ramped down.

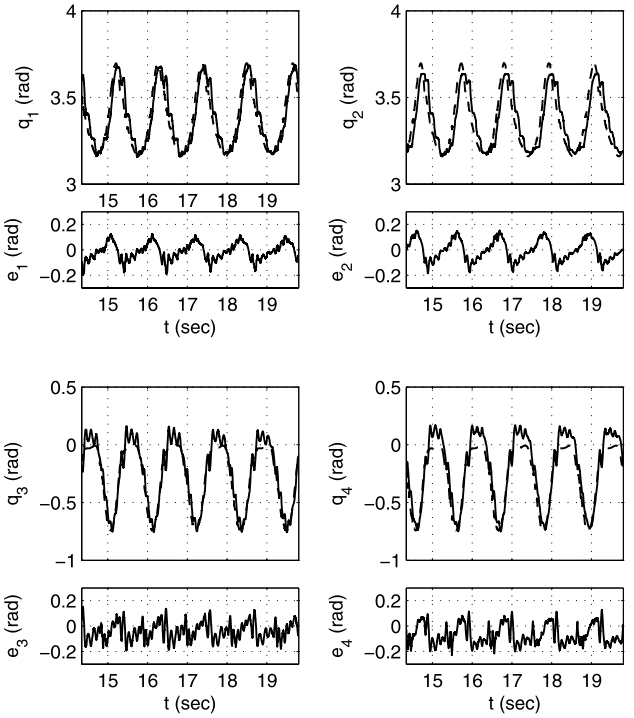

Fig. 8 Joint angles q_i and errors $e_i = q_i - h_{d,i}$, $i = 1$ to 4, versus time for ERNIE walking at 0.5 m/s with knee springs of equivalent stiffness 16 N m/rad and preload 2.74 N m. Measured joint trajectories are solid and $h_{d,i}$ for $i = 1, \ldots, 4$ are dashed. Since the legs of the physical robot alternate in their roles of stance and swing legs, the coordinates $q_1, \ldots, q_4$ in this figure are defined differently from Fig. 4. Here, q_1 and q_3 are the measured hip and knee joint angles of the leg farthest from the wall in Fig. 1, and q_2 and q_4 are the measured hip and knee joint angles of the leg nearest to the wall in Fig. 1

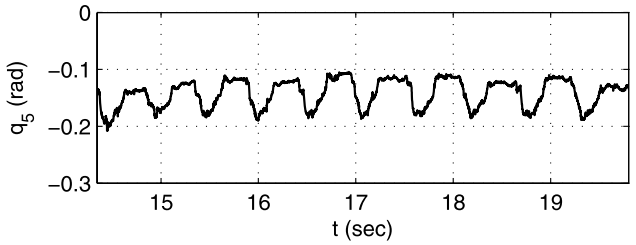

Fig. 9 Torso angle q_5 versus time for ERNIE walking at 0.5 m/s with knee springs of equivalent stiffness 16 N m/rad and preload 2.74 N m

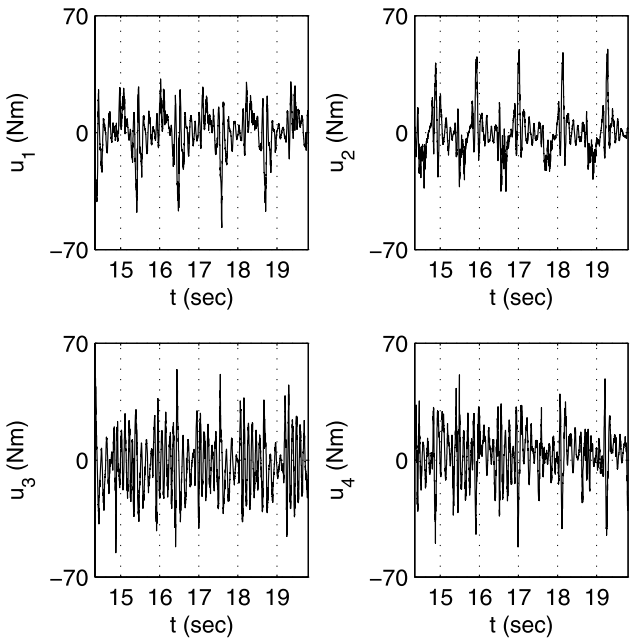

Fig. 10 Estimated torque versus time for ERNIE walking at 0.5 m/s with knee springs of equivalent stiffness 16 N m/rad and preload 2.74 N m

6.2 Experiment results

Walking tests were performed for the four cases, i.e., walking without springs and walking with the three different sets of springs with parameters given in Table 2. Each case has eight gaits corresponding to eight different average walking rates from 0.3 m/s to 0.65 m/s in increments of 0.05 m/s. A total of thirty-two tests were performed. Feedback controllers were designed using the corresponding gait obtained in Sect. 5 to induce stable walking at a desired average rate according to the given system configuration, i.e., without knee compliance or with different knee compliances. For each test, ERNIE was configured to walk on the treadmill, and data was collected for 20 seconds of steady-state walking.

Figures 8–10 are plots of various quantities of interest over a representative time interval containing approximately ten steps for the walking test with knee compliance of equivalent stiffness 16 N m/rad and preload 2.74 N m at a rate of 0.5 m/s. Figure 8 gives the joint trajectories and tracking errors for each hip and knee joint. The plots indicate good tracking, and hence, that the designed motion was enforced. Figure 9 gives the evolution of the torso angle. Note that although the torso angle was not directly controlled, its motion was periodic. Figures 8 and 9 together indicate that ERNIE walked with a periodic gait. Figure 10 gives the joint torques estimated from the measured current of each motor. The peak commanded torque is 62.5 N m, which is below the maximum torque the motor can supply, estimated to be approximately[1] 75 N m.

The average power cost for each test was calculated in a time window of approximately 20 seconds, which started from the first double support phase to the last double support phase of the data-recording period. The average power was based on the measured amplifier output current I_{AMP} using the standard relation between applied current and motor/gearhead output, $\tau = N k_t I_{AMP}$, where N is the gear ratio

[1] It is assumed that the ambient temperature is 25°C, and the maximum current is applied cyclically with a duty cycle of 20%.

and k_t is the motor torque constant. The average power cost P_{avg} was estimated by

$$P_{avg} = \frac{1}{T}\int_0^T \sum_{i=1}^{4} \left|\tau_i(t)\dot{q}_{m_i}\right| dt, \tag{20}$$

where, for $i = 1, \ldots, 4$, τ_i is the estimated motor torque, $\dot{q}_{m_i}$ is the gearhead output velocity calculated by differentiating the motor encoder signal, and T is the duration of the selected time interval.

The average power cost for each of the four cases versus walking rate is given in Fig. 11. It can be seen from this plot that the power cost trends with and without parallel knee compliance match the simulation results: at low speeds, the average power cost with knee compliance is higher than without knee compliance, and at higher speeds, the average power cost with knee compliance is lower than without knee compliance. Comparing Figs. 5(a) and 11(a), the average power cost found in the experiments is about three times the average power cost the designed gait. This difference is the result of imperfect modeling of the physical system and is not problematic given the agreement between the trends found in simulation and in experiment.

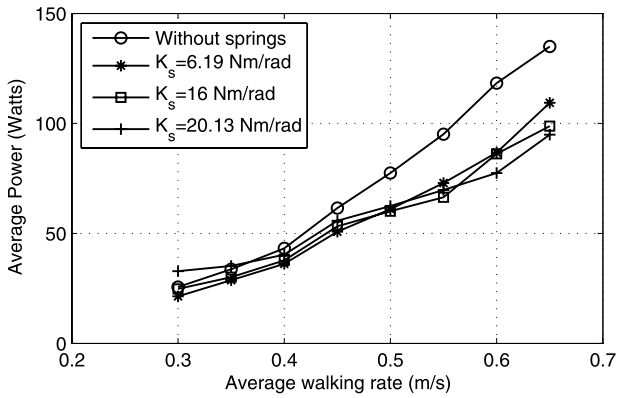

(a) Average power cost with and without springs for various speeds and spring stiffness

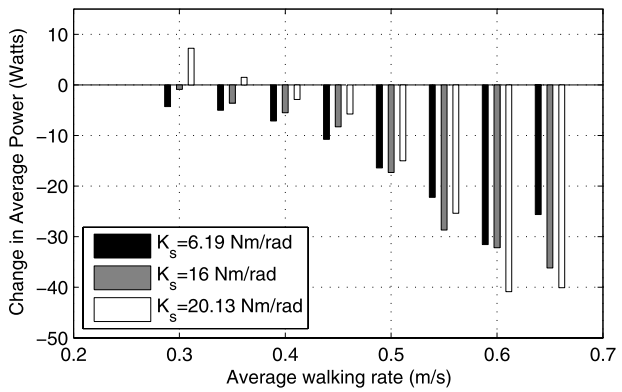

(b) Changes in average power cost with springs compared with the average power cost without springs

Fig. 11 Average power over one step calculated from experiments

7 Conclusion

This paper reports on the 5-link biped ERNIE designed, constructed, and housed at The Ohio State University. The paper also includes the results of a study of the effects of compliance added in parallel with the knee actuators. ERNIE has a number of important design features, including a modular leg design that makes it possible to change the leg's components with minimal mechanical modification, and a knee design that enables the addition of compliance in parallel with the knee actuators. The modular legs make it possible to easily test different foot designs, change leg length, etc. The ability to easily add parallel knee compliance facilitated the study of the effects of the added compliance.

Using parametric optimization, four sets of gaits were designed for a range of average walking rates. Among these four sets of gaits, one set was designed for walking without springs, and the other three were designed for walking with springs of different stiffness and preload. For each gait, the average power cost was computed numerically and evaluated experimentally on ERNIE. It was found that the addition of springs in parallel with the knee actuators can improve the energetic efficiency of walking, with higher stiffness providing greater benefit at higher speeds and lower stiffnesses providing benefit at lower speeds.

ERNIE will continue to serve as a testbed for the study of bipedal locomotion. Various studies are underway, including verification of the framework for aperiodic walk proposed in Yang et al. (2007) and a study of the effects of foot shape. Study of the effects of adding compliance at ERNIE's hips will also be investigated.

References

Ahmadi, M., & Buehler, M. (1999). ARL monopod II running robot: control and energetics, In *Proc. of the 1999 IEEE International Conference on Robotics and Automation*, Detroit, MI (vol. 3, pp. 1689–1694).

Alexander, R. M. (1999). Three uses for springs in legged locomotion. *International Journal of Robotics Research*, *9*(2), 53–61.

Anderson, S. O., Wisse, M., Atkeson, C. G., Hodgins, J. K., Zeglin, G. J., & Moyer, B. (2005). Powered bipeds based on passive dynamic principles. In *Humanoid Robots, 2005 5th IEEE-RAS International Conference* (pp. 110–116).

Bastien, G. J., Willems, P. A., Schepens, B., & Heglund, N. C. (2005). Effect of load and speed on the energetic cost of human walking. *European Journal of Applied Physiology*, *94*(1–2), 76–83.

Browning, R. C., & Kram, R. (2005). Energetic cost and preferred speed of walking in obese vs. normal weight women. *Obesity Research*, *13*(5), 891–899.

Capi, G., Nasu, Y., Barolli, L., & Mitobe, K. (2003). Real time gait generation for autonomous humanoid robots: a case study for walking. *Robotics and Autonomous Systems*, *42*(2), 107–116.

Channon, P. H., Hopkins, S. H., & Pham, D. T. (1992). Derivation of optimal walking motions for a bipedal walking robot. *Robotica*, *10*, 165–172.

Chevallereau, C., Abba, G., Aoustin, Y., Plestan, F., Westervelt, E. R., Canudas, C., & Grizzle, J. W. (2003). RABBIT: a testbed for advanced control theory. *IEEE Control Systems Magazine*, *23*(5), 57–79.

Chevallereau, C., & Aoustin, Y. (2001). Optimal reference trajectories for walking and running of a biped robot. *Robotica*, *19*(5), 557–569.

Chow, C. K., & Jacobson, D. H. (1971). Studies of human locomotion via optimal programming. *Mathematical Biosciences*, *10*, 239–306.

Coleman, M. J., & Ruina, A. (1998). An uncontrolled walking toy that cannot stand still. *Physical Review Letters*, *80*(16), 3658–3661.

Collins, S. H., & Ruina, A. (2005). A bipedal walking robot with efficient and human-like gait. In *Proc. of the 2005 IEEE International Conference on Robotics and Automation*, Barcelona, Spain (pp. 1983–1988).

Collins, S. H., Ruina, A., Tedrake, R., & Wisse, M. (2005). Efficient bipedal robots based on passive-dynamic walkers. *Science*, *307*, 1082–1085.

Collins, S. H., Wisse, M., & Ruina, A. (2001). A three-dimensional passive-dynamic walking robot with two legs and knees. *International Journal of Robotics Research*, *20*(7), 607–615.

Farrell, K. D., Chevallereau, C., & Westervelt, E. R. (2007). Energetic effects of adding springs at the passive ankles of a walking biped robot. In *Proc. of the 2007 IEEE International Conference on Robotics and Automation*, Rome, Italy (pp. 3591–3596).

Garcia, M., Chatterjee, A., & Ruina, A. (2000). Efficiency, speed, and scaling of two-dimensional passive-dynamic walking. *Dynamics and Stability of Systems*, *15*(2), 75–99.

Gunther, M., & Ruder, H. (2003). Synthesis of two-dimensional human walking: a test of the lambda-model. *Biological Cybernetics*, *89*(2), 89–106.

Hurst, J. W., Chestnutt, J. E., & Rizzi, A. A. (2007). Design and philosophy of the BiMASC, a highly dynamic biped. In *Proc. of the 2007 IEEE International Conference on Robotics and Automation*, Rome, Italy (pp. 1863–1868).

Iida, F., Minekawa, Y., Rummel, J., & Seyfarth, A. (2005). Toward a humanlike biped robot with compliant legs. *Intelligent Autonomous Systems*, *9*, 820–827.

Kato, I., & Tsuiki, H. (1972). The hydraulically powered biped walking machine with a high carrying capacity. In *Proc. of the Fourth International Symposium on External Control of Human Extremities*, Dubrovnik, Yugoslavia (pp. 410–421).

Kuo, A. D. (2007). Choosing your steps carefully. *Robotics & Automation Magazine, IEEE*, *14*(2), 18–29.

Loffler, K., Gienger, M., Pfeiffer, F., & Ulbrich, H. (2004). Sensors and control concept of a biped robot. *IEEE Transactions on Industrial Electronics*, *51*(5), 972–980.

McGeer, T. (1990). Passive dynamic walking. *Internarional Journal of Robotics Research*, *9*(2), 62–82.

Pratt, J. E., Chee, M. C., Torres, A., Dilworth, P., & Pratt, G. A. (2001). Virtual model control: an intuitive approach for bipedal locomotion. *International Journal of Robotics Research*, *20*(2), 129–143.

Pratt, J. E., & Pratt, G. A. (1998). Intuitive control of a planar bipedal walking robot. In *Proc. of the 1998 IEEE International Conference on Robotics and Automation*, Leuven, Belgium (pp. 2014–2021).

Raibert, M. H. (1986). *Legged robots that balance*. Cambridge: MIT.

Ralston, H. J. (1958). Energy-speed relation and optimal speed during level walking. *European Journal of Applied Physiology*, *17*(4), x–x.

Rostami, M., & Bessonnet, G. (1998). Impactless sagittal gait of a biped robot during the single support phase. In *Proc. of the 1998 IEEE International Conference on Robotics and Automation*, Leuven, Belgium (pp. 1385–1391).

Rostami, M., & Bessonnet, G. (2001). Sagittal gait of a biped robot during the single support phase. Part 2: optimal motion. *Robotica*, *19*, 241–253.

Saidouni, T., & Bessonnett, G. (2003). Generating globally optimised sagittal gait cycles of a biped robot. *Robotica*, *21*, 199–210.

Sakagami, Y., Watanabe, R., Aoyama, C., Matsunaga, S., Higaki, N., & Fujimura, K. (2002). The intelligent ASIMO: system overview and integration. In *Proc. of the 2002 IEEE/RSJ International Conference on Intelligent Robots and Systems*, Lausanne, Switzerland (pp. 2478–2483).

Tedrake, R. (2004). Applied optimal control for dynamically stable legged locomotion. PhD thesis, Massachusetts Institute of Technology.

Vanderborght, B., Verrelst, B., Van Ham, R., Van Damme, M., Lefeber, D., Meira Y Duran, B., & Beyl, P. (2006). Exploiting natural dynamics to reduce energy consumption by controlling the compliance of soft actuators. *International Journal of Robotics Research*, *25*, 343–358.

Westervelt, E. R., Buche, G., & Grizzle, J. W. (2004). Experimental validation of a framework for the design of controllers that induce stable walking in planar bipeds. *International Journal of Robotics Research*, *23*(6), 559–582.

Westervelt, E. R., Grizzle, J. W., Chevallereau, C., Choi, J. H., & Morris, B. (2007). *Feedback control of dynamic bipedal robot locomotion*. Taylor & Francis/CRC.

Westervelt, E. R., Grizzle, J. W., & Koditschek, D. E. (2003). Hybrid zero dynamics of planar biped walkers. *IEEE Transactions on Automatic Control*, *48*(1), 42–56.

Wisse, M., Schwab, A. L., van der Linde, R. Q., & van der Helm, F. C. T. (2005). How to keep from falling forward: Elementary swing leg action for passive dynamic walkers. *IEEE Transactions on Robotics*, *21*(3), 393–401.

Wisse, M., Schwab, A. L., & van der Linde, R. Q. (2001). A 3D passive dynamic biped with yaw and roll compensation. *Robotica*, *19*(3), 275–284.

Yang, T., Westervelt, E. R., & Serrani, A. (2007). A framework for the control of stable aperiodic walking in underactuated planar bipeds. In *Proc. of the 2007 IEEE International Conference on Robotics and Automation*, Rome, Italy (pp. 4661–4666).

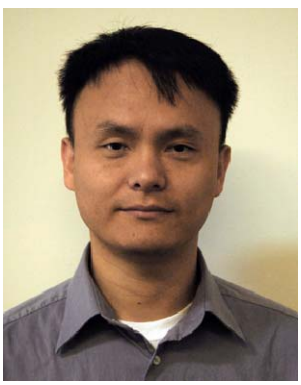

T. Yang received his B.S. degree from Zhejiang University, Hangzhou, China in 1998, and M.S. degree from Kansas State University, Manhattan, KS in 2004, both in mechanical engineering. Currently he is a Ph.D. candidate in mechanical engineering at The Ohio State University, Columbus, OH. From 1998 to 2001, he was with Shanghai Institute of Satellite Engineering as an engineer. His research interests include legged robot dynamics and control, and motion control systems.

E.R. Westervelt received the B.S. degree in computer and systems engineering from Rensselaer Polytechnic Institute, Troy, NY, and the Ph.D. degree in electrical engineering from the University of Michigan, Ann Arbor, in 1997 and 2003, respectively. From 2003 to 2007 he was an assistant professor in the Department of Mechanical Engineering at the Ohio State University. Since 2008 he has been a Control Systems Engineer in the Electronics and Energy Conversion Group at the General Electric Global Research Center, Niskayuna, NY. His research interests include the theory and practice of control as applied to mechanical systems.

J.P. Schmiedeler received the B.S. degree from the University of Notre Dame, Notre Dame, IN, in 1996, and the M.S. and Ph.D. degrees from The Ohio State University, Columbus, in 1998 and 2001, respectively, all in mechanical engineering. He was an Assistant Professor with the Department of Mechanical and Industrial Engineering, University of Iowa, Iowa City, from 2002 to 2003. Since fall 2003, he has been with The Ohio State University as an Assistant Professor with the Department of Mechanical Engineering. His research interests lie in machine design, kinematics, and dynamics as applied to the development of robotic systems. His current work focuses on legged robots and the biomechanics of human motion.

R.A. Bockbrader received his B.S. and M.S. degrees in mechanical engineering from The Ohio State University in 2004 and 2006, respectively. He is currently with Palmer Associates.